

JOURNAL OF ADVANCED APPLIED SCIENCES

e-ISSN: 2979-9759



RESEARCH ARTICLE

Characterization of 3-Chloro-4-Fluoronitrobenzene Molecule with New Calculation Methods and Discussions for Advanced Applied Sciences

Muhammed Oz^{1™} • Ali Serol Erturk² • Umit Erdem³

¹Bolu Abant Izzet Baysal University, Gerede Vocational School, Department of Chemistry and Chemical Processing Technology, Bolu/Türkiye

ARTICLE INFO

Article History

Received: 15.11.2024 Accepted: 06.12.2024 First Published: 30.12.2024

Keywords

Comparison

DFT HF

ICT Regions

Simulations



ABSTRACT

This current research characterizes 2-chloro-1-fluoro-4-nitrobenzene molecule via the Hartree Fock (HF) and density functional theory (DFT) quantum mechanical computational techniques using B3LYP/6-311++G(d,p) levels of computation. The molecular geometries, thermodynamic quantities at 300 K, NMR chemical shifts, corresponding vibrational spectra, UV-vis spectra, vibrational frequencies, and atomic point charge distributions are extensively investigated. The ¹H and ¹³C NMR chemical shifts, and theoretical vibrational frequencies are compared to the experimental results. It is obtained that all calculations are in agreement with the available experimental data which has the ¹H isotropic chemical shifts range from 8.306 ppm to 7.235 ppm, while the computed values range from 9.0368 ppm to 6.8397 ppm, 8.3213 ppm to 6.1242 ppm at DFT and HF GIAO levels, respectively. Besides, calculated ¹³C chemical shifts vary from 141.83 ppm to 186.394 ppm and from 129.743 ppm to 174.373 ppm by using DFT and HF in CH₄, while these values are in the range of 117.00 ppm to 164.59 ppm, experimentally. This points out that the chosen computation sets are highly effective methods for identifying and characterizing the compound. In addition, simulations are performed to examine frontier molecular orbitals, electrostatic potential, and molecular electrostatic potential regions. Key properties such as dipole moment, chemical hardness, transition states, electronegativity, molecular softness, nucleophilic aromatic regions, electrophilicity index, and energy band gap are also analyzed to explore potential future applications such as advanced applied sciences, industry, chemistry, medical, physics, biology, pharmaceuticals, dyes, and agrochemicals of the compound. Additionally, it is noted that the compound contains significant intramolecular charge transfer (ICT) regions, lone electron pairs, electron-donating groups, π -bond conjugation, and particularly reactive electrophilic and nucleophilic aromatic sites. Accordingly, it is pointed out that the molecule has a strong potential for metallic bonding as well as various intermolecular interactions. In summary, this study provides valuable information that will benefit both basic research and technological or industrial applications by increasing the understanding of physical, chemical, structural, and reactive features of the 3-chloro-4-fluoronitrobenzene molecule.

Please cite this paper as follows:

Oz, M., Erturk, A. S., & Erdem, U. (2024). Characterization of 3-chloro-4-fluoronitrobenzene molecule with new calculation methods and discussions for advanced applied sciences. *Journal of Advanced Applied Sciences*, 3(2), 40-54. https://doi.org/10.61326/jaasci.v3i2.311

1. Introduction

The compound with the molecular formula of C₆H₃ClFNO₂, 3-chloro-4-fluoronitrobenzene (sometimes called as 2-chloro-

1-fluoro-4-nitrobenzene) possesses a molecular weight of 175.54 g/mol. Especially, with the functional groups including chloro (Cl), nitro (NO₂), the fluoro (F) groups, the title

E-mail address: moz@ibu.edu.tr



²Adıyaman University, Faculty of Pharmacy, Department of Basic Pharmacy Sciences, Adıyaman/Türkiye

³Kırıkkale University, Kırıkkale Vocational School, Department of Electronics and Automation, Kırıkkale/Türkiye

[™] Correspondence

compound can find several application fields as a result of the usage of an intermediate in organic synthesis, especially in the production of pharmaceuticals, dyes, and agrochemicals. Besides, the organic compound with distinct functional groups including the valuable combination of a nitro group and two halogens (nitro, fluorine, and chlorine groups) makes the organic material studied reactive in electrophilic and nucleophilic aromatic substitution reactions and thus useful for further functionalization. This compound with a halogenated benzene ring is often used in pharmaceutical research in the case of the requirement of electron-withdrawing effects. The attractive crystal structure (high reactivity) allows selective modification in medicinal chemistry, particularly antimicrobial, anti-inflammatory, and anticancer drugs. Also, chlorine and fluorine contribute to the reactivity of molecules for designing molecules with specific binding affinity and metabolic stability. The presence of halogens (for better bonding to fibers and substrates) and a nitro group (for color stability) gives vibrant colors and improved adhesion. In polymer chemistry, the structure of 2-chloro-1-fluoro-4-nitrobenzene makes it ideal for creating polymers with enhanced thermal stability and resistance to degradation. As a polymer additive, it improves combustion resistance and flame-retardant properties. In agrochemicals, 3-chloro-4-fluoronitrobenzene developing plant protection products due to its strong electronwithdrawing properties and biological activity, making it useful for insecticides, herbicides, and fungicides.

Additionally, due to its reactivity, the 3-chloro-4fluoronitrobenzene compound has widely been used in organic research environments as a starting material, substrate, or functional group-bearing molecule to explore nucleophilic aromatic substitutions or further functionalization studies. The 3-chloro-4-fluoronitrobenzene molecule is also used to study unique substitutions, reaction mechanisms, or synthetic routes. However, although the 3-chloro-4-fluoronitrobenzene is a very valuable chemical substance in many application fields, it has not found a place in many studies. It is seen that six valuable articles are directly related to the 3-chloro-4fluoronitrobenzene in the literature. Namely, in a study performed in 2008, the reduction of heterocycles and fluorinecontaining nitroaromatics using microwave irradiation power of Mo(CO)6 and DBU in EtOH, the 2-chloro-1-fluoro-4nitrobenzene, which could play a crucial role in the other compound synthesis of biological molecules, was used as one of the starting materials to get various anilines (Spencer et al., 2008). In a 2024 study, researchers modified oxidized hydrogen-substituted graphyne and combined it with carbon nanotubes (CNTs) using seven ionic liquids through covalent and non-covalent bonding to investigate how ionic liquid structure and CNT incorporation mode impacted material properties, finding that longer alkyl chain ionic liquids had higher adsorption capacities and that CNT incorporation affected the dispersion and interaction with the genotoxic

3-chloro-4-fluoronitrobenzene impurity gefitinib. demonstrating an economical and simple method for impurity analysis (Zhang et al., 2024). Moreover, Chen and Wang (2021) performed detailed experimental investigations on the density, viscosity, and saturated vapor pressure features for the characterization of the 3-chloro-4-fluoronitrobenzene molecule. In 1997, Ravi et al. conducted experimental studies on the organic synthesis of the 3-chloro-4-fluoronitrobenzene molecule (Ravi et al., 1997). Besides, the molecule was used as a starting material for the production of phenylated diamine, bis(4-amino-2-biphenyl) ether (Morikawa et al., 2005). Moreover, a scientific study has been conducted to investigate changes in the toxicity of chemicals in water as a result of the use of solvents or dispersants as carriers in 2016 (Kikuchi et al., 2016). The research group was used to investigate the bioavailable concentration of the test chemical and whether the compound had a significant or minimal effect on the acute toxicity of the chemical. At the same time, quantum chemistry modeling approaches are powerful tools for predicting the fundamental features of organic molecules and offering deeper insights into experimental phenomena.

In the current study, we perform full identification of the 2chloro-1-fluoro-4-nitrobenzene molecule with the aid of quantum chemistry models such as HF and DFT within B3LYP and 6-311++G(d,p) computation technique. The theoretical predictions extracted from the modern calculation methods are compared to the experimental observations in the SDBS (10089) database (Ertem & Altunpak, 2019), assessing a strong correlation between theoretical and experimental data for vibrational frequencies deduced from FTIR spectra and NMR spectra. A detailed analysis is conducted on the UV-visible (UV-vis) spectra and a range of thermodynamic properties including heat capacity, total/zero-point vibrational/thermal energy, rotational constants, total dipole moments, and entropy belonging to the 3-chloro-4-fluoronitrobenzene compound. Furthermore, atomic charge distributions are examined to assess dipole moments and regions of intramolecular charge transfer (ICT). The study reveals that the title molecule with the electrophilic and nucleophilic aromatic regions shows potential for metallic bonding and strong intermolecular interactions. It should be referred here that the presence of intramolecular charge transfers enables the compound to be used in the electrode materials (Altunpak et al., 2019; SDBS, 2024). At the same time, this research includes visualization of key electronic properties, such as MEP, LUMO, ESP, and HOMO images providing detail information about electrophilicity, transition states, nucleophilic aromatic regions, chemical hardness, energy band gaps, molecular softness, and electronegativity so that we can understand the high reactivity of the sample studied for the future application fields as regards advanced applied sciences, physics, industry, chemistry, biology, medical, pharmaceuticals, dyes, and agrochemicals of the compound.

2. Materials and Methods

This study provides comprehensive computational analyses including optimized molecular geometry, atomic charges, dipole moment, vibrational frequencies, ICT regions, Raman activities, thermodynamic properties at 300 K, UV-vis spectra, functional group identifications, charge transfer characteristics, NMR chemical shifts utilizing from Gaussian 09 package (Dennington et al., 2007) and molecular visualization program (Becke, 1992; Stephens et al., 1994; Wu & Yang, 2002) at B3LYP method by 6-311++G(d,p) set (Saiardi et al., 1999; Schell et al., 1999) embedded in HF and DFT quantum computational technique of 3-chloro-4-fluoronitrobenzene compound, as shown in Figure 1, for the first time. Electronic properties are analyzed through MEP, LUMO, HOMO, and ESP mappings, while energy band gaps and transition states are evaluated to understand the stability, reactivity, and potential applications of the 2-chloro-1-fluoro-4-nitrobenzene molecule.

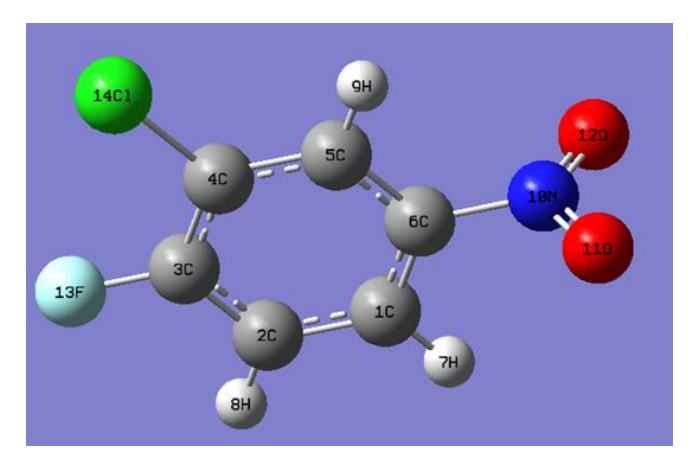


Figure 1. Molecular geometries of 3-chloro-4-fluoronitrobenzene molecule.

This work provides a quality reference on the physical, chemical, structural, and electronic characteristics of the 3-chloro-4-fluoronitrobenzene compound for future studies. Additionally, theoretical NMR shifts are calculated using the B3LYP/6-311++G(d,p) basis level set with the Gauge-Including Atomic Orbital (GIAO) method. Visible electronic absorption maxima are determined using the quantum mechanical methods of TDF/DFT, CIS, and TDF/HF (Furche & Ahlrichs, 2002). Theoretical force constants in Cartesian coordinates are determined under the Cs point group for the optimized geometry. The force field (Pulay et al., 1983; Rauhut & Pulay, 1995) is adjusted through selective scaling within the internal coordinates (Fogarasi & Pulay, 1986; Fogarasi et al., 1992; Keresztury et al., 1993; Polavarapu, 1990).

The electronic features are further analyzed based on total energy calculations and Koopmans' theorem principles. The ionization potential (IP) is calculated by comparing the energy of the radical cation formed by electron loss with that of the neutral molecule and also gives valuable information about the ionization tendency and electronic behavior of the molecule (Buyukuslu et al., 2010). One can see the following relations:

$$IP_{TE} = E_{cation} - E_n$$
 (1)

$$IP_{KE} = -E_{HOMO}$$
 (2)

Additionally, EA indicates the electron affinity with the aid of energy differentiation between the anion and neutral molecules:

$$EA_{TE}=E_n-E_{anion}$$
 (3)

$$EA_{KE} = -E_{LUMO}$$
 (4)

The IP and EA (electron affinity) are utilized to determine key thermodynamic and physical properties, including electronegativity (χ), softness (ζ), electrophilicity index (ψ), and hardness (η) coefficients (Kohn et al., 1996; Politzer & Abu-Awwad, 1998). Chemical hardness and electronegativity are then found by the corresponding formulas of 5 and 6.

$$\mu \approx -\gamma = -(IP + EA)/2 \tag{5}$$

$$\eta \approx (IP-EA)/2$$
 (6)

Moreover, the softness and electrophilicity indices are determined by using 7 and 8. Namely,

$$\zeta = 1/(2\eta) \tag{7}$$

$$\Psi = (\mu 2/2\eta) \tag{8}$$

3. Results

In this work, we are interested in the vibrational frequencies, related assignments of vibrations, optimized molecular structures, atomic charge distributions, dipole moments, ICT regions, thermodynamic properties (rotational constants, entropy, heat capacity, and scaled zero-point vibrational/thermal/total energies) at 300 K, UV-vis absorption maxima, functional group identifications, electrophilic/nucleophilic aromatic regions, charge transfer characteristics, lone (non-bonding) pairs, chemical hardness, energy band gap, molecular softness, and electronegativity NMR chemical shifts, conjugation of π bonds, electron engagement, 2D total charge contours, MEP, LUMO, ESP, and HOMO images of 3-chloro-4-fluoronitrobenzene compound for the first time.

The illustration of 3-chloro-4-fluoronitrobenzene molecule is depicted in Figure 1. The related geometric parameters including bond length sizes and bond angles of 3-chloro-4-fluoronitrobenzene molecule performed by both DFT and HF computation levels of theory are given in Table 1. Prior to the crucial discussions, Table 1 strongly indicates that all the bond lengths and both angles are found to be in perfect agreement with each other. That is exactly why the modern calculation methods preferred in the current work are reliable. In detail, two models show that there are no distortions and deviations in the bond length sizes and bond angles on the benzene ring. The

carbon and carbon bond lengths are calculated as 1.4014 Å and the lengths for C-H bonds are calculated to be 1.07 Å at both calculation methods. Similarly, the C-F bond length sizes are calculated to be 1.35 Å when the length between the nitrogen and carbon atoms is obtained to be 1.47 Å. Besides, the bond length size between nitrogen and oxygen atoms is computed to be 1.35 Å. Likewise, the bond angles are not distorted. On this basis, the bond angles between carbons is computed as 1200. Moreover, the bond angle between carbon-carbon-fluorine, or chlorine atoms and carbon-carbon-hydrogen atoms is calculated to be 1200. Also, the bong angle between carbons and nitrogen atoms is found to be 109.39690. Further, the angle for carbon-nitrogen-oxygen atoms is determined to be 109.39690. Additionally, the bond angle between oxygennitrogen-oxygen atoms is obtained as 106.54840 (Table 1). The perfect harmony between the calculated structural geometry parameters shows us that the DFT and HF quantum mechanical methods can be used to determine all other features. Shortly, the title 3-chloro-4-fluoronitrobenzene molecule with distinct functional groups has an ideal geometry for electrophilic and nucleophilic interactions.

The studied molecule (C_s point group) possesses 14 atoms, hence, there appears an identity and a reflection plane symmetry element. There are 3N internal vibrational modes (Wilson et al., 1980) resulting from the three Cartesian

displacements. Among them, six modes account for translational and rotational movements. Therefore, the remaining 36 (3N-6) modes are characterized as 22 A' and 14 A" modes. In the Raman spectra, the A' modes, representing symmetric (in-plane) vibrations, are polarized, while the A" modes, which correspond to anti-symmetric (out-of-plane) vibrations, are depolarized (Krishnakumar et al., 2008). The spectroscopic features of the 3-chloro-4-fluoronitrobenzene molecule are extensively examined through frequency calculation analysis. Detailed vibrational assignments for the fundamental modes are provided in Table 2, offering insights into their structural and spectroscopic behaviors.

The presence of aromatic rings can be readily identified through the characteristic vibrations related to the C–C and C–H rings. The stretching vibrations of C–H bonds occur above 3000 cm⁻¹ and typically appear as a series of weak to moderate bands, in contrast to the aliphatic C–H stretching modes (Coates, 2006). In the current work, the stretching frequencies are calculated between 3195 cm⁻¹ and 3220 cm⁻¹ and 3217 cm⁻¹ and 3251 cm⁻¹ at DFT and HF calculation basis sets, respectively. The experimental findings are determined to vary between 3427 cm⁻¹ and 2925 cm⁻¹ under different solvents. As for the benzene ring vibrations, the C=C stretching modes are calculated to be about 1504 cm⁻¹ and 1586 cm⁻¹ using the quantum mechanical calculation methods.

Table 1. Theoretical geometric (bond lengths and angles) parameters of the 3-chloro-4-fluoronitrobenzene molecule.

	Bond Length	Bond Angles (°)			
Elements	DFT/B3LYP//6-311++G(d,p)	HF/6-311++G(d,p)	Elements	DFT/B3LYP//6-311++G(d,p)	HF/6-311++G(d,p)
C1-C2	1.40	1.40	C2-C1-C6	120.0	120.0
C1-C6	1.40	1.40	C2-C1-H7	120.0	120.0
C1-H7	1.07	1.07	C6-C1-H7	120.0	120.0
C2-C3	1.40	1.40	C1-C2-C3	120.0	120.0
C2-H8	1.07	1.07	C1-C2-H8	120.0	120.0
C3-C4	1.40	1.40	C3-C2-H8	120.0	120.0
C3-F13	1.35	1.35	C2-C3-C4	120.0	120.0
C4-C5	1.40	1.40	C2-C3-F13	120.0	120.0
C4-Cl14	1.76	1.76	C4-C3-F13	120.0	120.0
C5-C6	1.40	1.40	C3-C4-C114	120.0	120.0
C5-H9	1.07	1.07	C5-C4-C114	120.0	120.0
C6-N10	1.47	1.47	C1-C6-N10	109.4	109.4
N10-O11	1.36	1.36	C6-N10-O12	109.4	109.4
N10-O12	1.36	1.36	O11-N10-O12	106.55	106.55

The stretching vibrational modes of N=O bonds are experimentally measured to be about 1674-1669 cm⁻¹. Similarly, these modes appear at 1642-1366 cm⁻¹ and 1752-1476 cm⁻¹ at DFT and HF levels of calculation, respectively. Moreover, the stretching modes for the fluorine and chlorine atoms are calculated as 1248-722 cm⁻¹ at the calculation levels. Experimentally, the stretching mode of F-C bonding is

measured to be about 1171 and 722 cm $^{-1}$. The other skeleton modes are found to be in a range of 46-1617 cm $^{-1}$ at DFT/B3LYP//6-311++G(d,p) basis set and 45-1699 cm $^{-1}$ HF/6-311++G(d,p) calculation levels. One can see similar results in the scientific studies (Baraistka et al., 1987; Rintoul et al., 2008; Wojtkowiak & Chabanel, 1977).

Table 2. Experimental and theoretical vibrational frequencies (cm⁻¹) for the 2-chloro-1-fluoro-4-nitrobenzene molecule.

	$({f r}^4) DFT$	r-1) HF			id Film)	Disc)	I mull)
Assignments	Scaled Freq. $({ m cm}^{-1})$ DFT	Scaled Freq. $(\mathrm{cm}^{\text{-1}})$ HF	IR Intent DFT	IR Intent HF	Exp. Freq. (Liquid Film)	Exp. Freq. (KBr Disc)	Exp. Freq. (nujol mull)
Usym(C-H)	3220.10	3251.59	11.35	10.93	3427	3411	2976
Usym(C-H)	3219.96	3248.80	6.59	5.49	2983		2951
Vasym(C-H)	3195.11	3217.75	0.03	0.12	2946	2949	2925
$v_{a+} v(_{O=N})$	1642.26	1751.54	29.36	390.29	1894	1757	1674
$\upsilon_{a+} \ \gamma_{(C-H)+} \ \upsilon_{(O=N)}$	1617.32	1699.31	50.90	90.43	1835	1655	1669
$v(_{O=N)+} v_{a+} y(_{C-H})$	1580.87	1682.23	253.37	194.21	1655		
$y(_{C-H)}+v(_{C=C)}+v(_{C3-F13})+v(_{C6-N10})$	1504.40	1586.08	125.38	37.34	1649		
$v_{a+} \gamma_{(C-H)}$	1423.22	1547.02	3.03	463.68	1468	1468	1464
v(O=N)+ y(C-H)+ v(C6-N10)	1365.50	1476.02	313.04	8.01	1379	1380	
$v_{asym} a + v_{(C-H)}$	1339.56	1340.12	22.67	99.64	1370	1370	1373
$B_a + \gamma_{(C-H)+} v_{(F-C)}$	1274.69	1307.72	123.35	4.15			
$B_a + \gamma_{\rm (C-H)}$	1251.40	1226.84	17.21	18.32			1249
γ (C-H)+ v (F-C)+ v (C6-N10)	1141.67	1192.73	37.37	16.96	1167	1168	1171
$B_a + \gamma_{(\text{C-H})+} \upsilon_{(\text{C6-N10})} + \upsilon_{(\text{F-C})}$	1126.18	1150.14	46.08	5.17	1150	1140	1126
$v_a + v_{(C-H)}$	1063.36	1108.71	27.16	3.15	1112	1111	1112
Φ (C-H)	971.87	1043.68	0.02	0.45	1004	1006	1009
O (C-H)	914.76	989.19	24.63	20.65	950	950	978
$B_a + \upsilon_{\rm (C6-N10)} + \gamma_{\rm (C-H)} + \upsilon_{\rm (F-C)}$	907.91	960.17	37.65	33.25			
U (С-H)	842.77	900.89	25.98	34.00	864	885	847
$\Phi_{ ext{molecule}}$	822.76	865.88	4.70	8.05	830	831	832
γ (C-C-C)+ ν (F-C)+ γ (O-N-O)	722.38	777.501	55.70	33.78			722
$\Phi_{ ext{molecule}}$	720.85	751.29	19.25	70.77			
Omolecule	695.56	742.33	0.40	0.14	671	672	
У (С-С-С)+ У (С-С-N)	641.75	666.64	13.30	20.18		611	640
γ (C-C-N)+ γ (C-C-F)+ γ (C-C-Cl)	557.32	579.31	1.19	1.44	556	558	
Omolecule	531.63	549.66	0.72	1.58			
$\gamma_{\text{(C-C-F)}}$ + $\gamma_{\text{(C-C-O)}}$ + $\gamma_{\text{(C-C-Cl)}}$	500.75	521.16	6.6	8.38	505		518
Oring+ γ (C-C-Cl) + γ (C-C-F)	450.13	475.36	3.57	4.47	441		
$\gamma(\text{C-C-C})+ \gamma(\text{C-C-N})+ \gamma(\text{C-C-F})$	367.42	380.39	0.11	0.01			
$\gamma_{\text{(C-C-C)}}$ + $\gamma_{\text{(C-C-H)}}$ + $v_{\text{(C-NO2)}}$	349.42	365.98	0.29	0.40			
Omolecule	327.80	347.75	0.24	0.29			
$\gamma_{\text{(C-C-CI)}} + \gamma_{\text{(C-C-F)}} + \gamma_{\text{(C-C-N)}}$	250.82	263.05	2.11	3.25			
$\gamma(\text{C-C-F})+\gamma(\text{C-C-N})+\gamma(\text{C-C-C})$	175.54	183.43	1.66	2.32			
Umolecule	169.16	178.94	0.02	0.07			
Umolecule	114.31	122.97	4.75	5.92			
ΨNO2+Wring	45.91	44.62	0.06	0.08			

Abbreviations used: \mathbf{y} . bending; \mathbf{w} . wagging; \mathbf{v} . stretching; \mathbf{sym} . symmetric; \mathbf{B} . breathing; \mathbf{v} . rocking; \mathbf{v} . torsion; \mathbf{asy} . asymmetric; $\mathbf{\phi}$. Twisting, \mathbf{o} : out of bending, and \mathbf{a} – Ring.

4. Discussion

In this study, atomic point charge distributions across the title 2-chloro-1-fluoro-4-nitrobenzene molecule are analyzed using the Mulliken population analysis method (Foresman & Frish, 1996; Helgaker et al., 1986; Olsen & Jørgensen, 1985) based on the quantum mechanical calculation method. For the level of calculations, both DFT and HF levels are used, and one can see atomic charges for each atom in Table 3. It is observed that the results obtained from both quantum computational methods are found to be in good agreement with each other. As for Mulliken carbon atomic charges, it is seen that the parameters are found to be both positive and negative. In this respect, the C4 atom possesses the maximum Mulliken value of 0.818936 a.u. at the DFT and 1.094944 a.u. at HF calculation levels due to its place closer to the ICT regions and lone pairs whereas the minimum value of -1.283815 a.u. and -1.246466 a.u. is computed at the B3LYP and HF levels of theory, respectively, for the C6 atom on the molecule. The Mulliken atomic point charge distributions for the nitrogen atom for the molecule are noted to be negative. That is -0.140476 a.u. and -0.067920 a.u. at the B3LYP and HF levels of theory, respectively. It can be attributed to a result of the intrinsic high electronegativity of the nitrogen atom. As for the distinct functional groups including halogens, the atomic charge of fluorine atoms is computed to be about -1.283815 a.u. and -1.246466 a.u.

The negatively charged lone pair verifies that charge is transferred from the carbon atom to the fluorine one. Thus, the fluorine atom behaves as the electron-withdrawing part of the molecule. In other words, this atom augments the functionalization and reactivity of the studied molecule so that the compound can be used for designing molecules with specific binding affinity and metabolic stability. Conversely, chlorine atoms lose electrons due to the position and charge transfer from carbon to chlorine atoms. Accordingly, the computationl methods calculate the high positive Mulliken values. Namely, the atomic charge for the chlorine on the molecule is calculated to be about 0.383411 and 0.286061 a.u. at the B3LYP and HF levels of theory. At the same time, both the oxygen atoms are calculated in negative values due to the acceptance of electrons (electron-withdrawing) along the molecule. Numerically, the DFT method calculates the values of -0.009972 a.u. for the O11 atom and -0.007071 a.u. for the O12 atom while the atoms are determined as -0.059361 a.u. and -0.062761 a.u. at HF modern computation method. As expected, all the hydrogen atoms lose the electron on the molecule. The highest Mulliken hydrogen atomic charge is determined to be about 0.282926 a.u. and 0.335952 a.u. for the H9 atom due to high negative charges around the atom and high electron engagement. All in all, the charge migrations are related to molecular interactions across the title compound. The presence of ICT regions, lone pairs, electron-donating groups, π-bond conjugation, and especially electrophilic/nucleophilic

aromatic regions based on the functional groups leads to the different distributions of atomic point charges across the compound studied. That is exactly why the material can be used in many advanced applied sciences. The variations between HF and B3LYP results can be attributed to factors such as π -conjugation within the carbon ring, the presence of nonbonding lone pairs, electron engagement, and ICT effects; nonetheless, the results remain largely consistent.

Table 3. Atomic point charge distributions across the 2-chloro-1-fluoro-4-nitrobenzene molecule.

Labe	l DFT/B3LYP//6-311++G(d,p)	HF/6-311++G(d,p)
C1	0.556907	0.433912
C2	-0.211351	-0.139069
C3	-0.889484	-1.059805
C4	0.818936	1.094944
C5	0.136082	0.070027
C6	-1.283815	-1.246466
H7	0.272392	0.317739
H8	0.223312	0.268211
H9	0.282926	0.335952
N10	-0.140476	-0.067920
O11	-0.009972	-0.059361
O12	-0.007071	-0.062761
F13	-0.131795	-0.171466
Cl14	0.383411	0.286061

transitions in the 2-chloro-1-fluoro-4-Electronic nitrobenzene molecule are classified by the orbitals involved and specific regions within the molecule. The two primary transitions observed are $\pi \to \pi^*$ (donor to acceptor), generally stronger, on the other hand, the transition of $n \to \pi^*$ is relatively weaker. To characterize the transitions, electronic absorption spectra are calculated using CIS, TD-DFT/B3LYP//6-3116+G(d,p), and TD-HF/6-311++G(d,p) levels of calculation in vacuum. In the computational approaches provided, there are some values for absorption maxima (λ), excitation energies, CIexpansion coefficients, oscillator strengths (f), singlet states, and main transition details, summarized in Table 4. It appears that all the calculation methods exhibit similar results for all the values. In the table, the λ parameter corresponds to electron availability, and key electronic transitions take places between frontier molecular orbitals. For excited state 1, transitions stem from HOMO-2 to LUMO, or HOMO-1→LUMO+14 or HOMO-2→LUMO+3 are identified, while additional transitions are detailed in Table 4.

Numerically, the calculated maximum absorption wavelengths (λ_{max}) are approximately 867.97 nm, 1665.41 nm, and 1226.17 nm for excited state 1 at the standard CIS, TD-DFT/B3LYP//6-311++G(d,p), and TD-HF/6-311++G(d,p) levels of calculation, respectively. For excited state 2, λ_{max}

parameters are found to be 482.25 nm, 756.14 nm, and 555.33 nm within the same calculation methods. Besides, for excited state 3, the λ_{max} values are calculated to be about 374.32 nm, 607.34 nm, and 497.25 nm at the calculation levels of CIS, TD-DFT/B3LYP//6-3116+G(d,p), and TD-HF/6-311++G(d,p),

respectively. 867.97 nm (1665.41 nm and 1226.17 nm) transition correspond to a $\pi \to \pi^*$ transition associated with C=C bonds, while 482.25 nm (756.14 nm and 555.33 nm) peak involves overlapping $\pi \to \pi^*$ transitions within the benzene ring, influenced by oscillation effects (Table 5).

Table 4. Theoretical electronic absorption spectra parameters inferred from CIS basis set.

CI-Expansion Coefficient						
Excitations	Energy (eV)	Singlet-A	Wavelength (nm)	Oscillator strength (f)	Translations	
Excited State 1						
39→45		-0.41940			HOMO-2→LUMO	
40→45		0.47988			HOMO-2→LUMO+1	
42→45	1.4284	-0.18942	867.97	0.0004	HOMO-2→LUMO+14	
43→45		0.12941			HOMO-1→LUMO	
4445		-0.12089			HOMO-1→LUMO+14	
Excited State 2						
37→45		0.10163	482.25		HOMO-2→LUMO	
38→45	2.5710	0.12234		0.0018	HOMO-2→LUMO+1	
<u>41→45</u>		-0.13039			HOMO-2→LUMO+3	
Excited State 3						
30→45		-0.13024			HOMO-2→LUMO	
36→45		-0.19514			HOMO-2→LUMO+1	
42→45	3.0417	-0.18573	374.32	0.0491	HOMO-2→LUMO+3	
43→45		-0.10329			HOMO-2→LUMO+14	
44→45		0.21455			HOMO-1→LUMO	

Table 5. Theoretical electronic absorption spectra parameters deduced from TD-DFT/B3LYP//6-3116+G(d,p), and TD-HF/6-311++G(d,p) calculation levels.

TD-DFT/B3LYP//6-3116+G(d,p)					
Excitations	Energy (eV)	Singlet-A	Wavelength (nm)	Oscillator strength (f)	Translations
Excited State 1					
41→45		0.11875			HOMO-3-LUMO
42→45	0.7445	-0.28750	1,665,41	0.0000	HOMO-2→LUMO
43→45	0.7445	-0.39962	1665.41	0.0000	HOMO-1→LUMO
44→45	0.506				HOMO→LUMO
Excited State 2					
41→45		-0.11746	756.14		HOMO-3→LUMO
42→45	1.6397	0.22109		0.0006	HOMO-2→LUMO
43→45	1.0397	0.43544			HOMO-1→LUMO
44→45		0.49338			HOMO→LUMO
Excited State 3					
41→45		-0.14123			HOMO-3→LUMO
42→45	2.0414	0.56931	607.34	0.0005	HOMO-2→LUMO
43→45		-0.38833			HOMO-1→LUMO
TD-HF/6-311++0	G(d , p)				

Table 5. (continued).

Excitations	Energy (eV)	Singlet-A	Wavelength (nm)	Oscillator strength (f)	Translations
Excited State 1					
39→45		-0.43665			HOMO-5→LUMO
40→45	1.0111	0.48435	1226.17	0.0003	HOMO-4→LUMO
42→45	1.0111	-0.24334	1220.17	0.0003	HOMO-2→LUMO
43→45		0.10265			HOMO-1→LUMO
Excited State 2					
37→45		0.15665	555.33		HOMO-7→LUMO
38→45	2.2326	0.66205		0.0015	HOMO-6→LUMO
41→45		-0.11241			HOMO-3→LUMO
Excited State 3					
42→45		0.50585			HOMO-2→LUMO
43→45	2.4934	0.22326	497.25	0.0403	HOMO-3→LUMO
44→45		-0.36931			HOMO→LUMO

A weak absorption peak of 374.32 nm (607.34 nm and 497.25 nm) corresponds to an $n \to \pi^*$ transition involving NO_2 and related halogen groups. In the CIS calculation method, oscillator strengths of 0.0004, 0.0018, and 0.0491 for these transitions are also shown in Table 4. The higher oscillator strength is observed for the weak absorption peak.

In the current work, we make NMR analyses for ¹³C and ¹H NMR spectra to identify the sample using the experimental and theoretical data using HF and B3LYP modern calculation techniques as a result of the perfect agreement between all the data discussed above. It is received that the latter calculation methods show much closer results due to electron correlation effects along the calculations. Even, B3LYP calculations for the vibrational spectra in the optimized molecular structure of the

molecule have already displayed a strong correlation with experimental data. In this study, the GIAO method for two quantum mechanical calculations is employed to calculate the ¹³C and ¹H NMR chemical shifts for the 3-chloro-4-fluoronitrobenzene molecule. One can see every calculation in Table 6. Experimentally, ¹H isotropic chemical shifts range from 8.306 ppm to 7.235 ppm, while the computed values range from 9.0368 ppm to 6.8397 ppm, 8.3213 ppm to 6.1242 ppm at DFT (B3LYP/6-311++(d,p))//TMS+HF/6-31G(d) GIAO and B3LYP/6-311++(d,p))//TMS+B3LYP/6-311+G(2d,p) GIAO levels of theory. The highest/smallest ¹H chemical shift is observed for the H9/H7 atom. It is normal to possess the maximum NMR chemical shift of the H₉ atom because of the highly electronegative atoms around the atom (the presence of ICT regions, lone pairs, and electron-donating groups).

Table 6. ¹³C and ¹H isotropic chemical shifts (concerning TMS, all values in ppm).

	DFT(B3LYP/	6-311++(d,p))//		HF(6-311++(d,p))//		Experimental
Label	TMS HF/6- 31G(d) GIAO	TMS B3LYP/6- 311+G(2d,p) GIAO	CH4 HF/6- 31G(d) GIAO	TMS HF/6- 31G(d) GIAO	TMS B3LYP/6- 311+G(2d,p) GIAO	CH4 HF/6- 31G(d) GIAO	CDCl ₃
C ₃	187.28	169.76	186.394	175.259	157.739	174.373	164.59
C_1	184.585	167.066	183.700	161.730	144.21	160.844	159.40
C_4	158.218	140.699	157.333	141.082	123.563	140.197	144.42
C_6	157.138	140.218	156.852	178.288	160.769	177.403	126.78
C_5	146.042	128.522	145.157	142.526	125.006	141.641	124.18-122.46
C_2	142.715	125.195	141.83	130.628	113.108	129.743	117.47-117.00
H_9	9.0368	8.3213		9.4301	8.7146		8.306
H_8	7.5097	6.7942		7.626	6.9105		7.424
H_7	6.8397	6.1242		5.898	5.1825		7.235

As for the HF quantum mechanical method results, ¹H chemical shifts are found to be in a range of 9.4301 ppm to 5.898 ppm, 8.7146 ppm to 5.1825 ppm at HF (6-

311++(d,p))/TMS+HF/6-31G(d) GIAO) and 6-311++(d,p))//TMS+B3LYP/6-311+G(2d,p) GIAO) calculation levels. In this respect, theoretical predictions (especially DFT

ones) observed from all the used methods demonstrate close agreement between experimental findings. For ¹³C NMR shifts relative to TMS, computed values span 142.715 ppm (C2) to 187.28 ppm (C3) at DFT (B3LYP/6-311++(d,p))//TMS+HF/6-31G(d) GIAO), 125.195 ppm to 169.760 ppm using B3LYP/6-311++(d,p))//TMS+B3LYP/6-311+G(2d,p) GIAO) levels of theory, compared to experimental shifts of 117.00 ppm to 164.59 ppm. Additionally, the chemical shifts for the carbon atoms are found to change from 130.628 ppm (C2) to 175.259 ppm (C3), 157.739 ppm to 113.108 ppm at HF (6-311++(d,p))/TMS+HF/6-31G(d)GIAO) and 311++(d,p))/TMS+B3LYP/6-311+G(2d,p) GIAO) calculation levels, respectively. Besides, ¹³C chemical shifts are calculated to vary from 141.83 ppm until 186.394 ppm and from 129.743 ppm to 174.373 ppm by using DFT (B3LYP/6-311++(d,p))//CH4 HF/6-31G(d) GIAO) and HF (6-311++(d,p))//CH4 HF/6-31G(d) GIAO) modern calculation methods. According to the theoretical calculations, it is observed that the DFT method calculates higher values than those of HF calculation level. In general, similar to other sections, it is stated that the DFT theoretical calculation method (especially DFT (B3LYP/6-311++(d,p))//TMS+HF/6-31G(d) GIAO)) offers the closest chemical shifts among the methods.

In the present study, thermodynamic properties including thermal energies, total, zero-point vibrational energy, heat capacities, rotational constants, entropies, and dipole moments (μ , μ_x , μ_y , μ_z , and μ) are computed using B3LYP and HF computational techniques. The calculated results are summarized in Table 7. It is seen that the zero-point vibrational energy (scaled by a valuable factor based on overestimation of harmonic vibrational frequencies (Avci & Atalay, 2009) is calculated to be about 52.078759764 a.u./Particle and 51.2612766 a.u./Particle at the DFT and the HF levels of theory. As for the total energy parameter, it is calculated as approximately -995.75777428 a.u. by the DFT quantum mechanical method, while the total energy is determined as -

992.07996302 a.u. by the HF modern calculation method. At the same time, total entropy values are approximately 95.275 cal.mol⁻¹K⁻¹ and 93.003 cal.mol⁻¹K⁻¹ at the B3LYP and HF levels, respectively. The thermal energy values are found to be 58.709 kcal.mol⁻¹ (B3LYP) and 62.827 kcal.mol⁻¹ (HF). Similarly, the total heat capacity values are determined to be approximately 32.620 cal.mol⁻¹K⁻¹ and 30.311 cal.mol⁻¹K⁻¹ at the B3LYP and HF calculation levels. The rotational constant values are calculated as 1.84572 GHz, 0.60797 GHz, and 0.45733 GHz at the DFT/B3LYP//6-311++G(d,p) level of theory, while the values are defined to be about 1.88353 GHz, 0.62104 GHz, and 0.46705 GHz at the HF/B3LYP//6-311++G(d,p) basis set.

The dipole moment, reflecting the uneven charge distribution across a molecule, plays a crucial role in analyzing intermolecular interactions, such as van der Waals forces, where higher dipole moments often correspond to stronger interactions. This parameter also provides insights into the formation of herbicides and insecticides and related biological properties of the molecule, particularly regarding interactions with enzyme active sites, and its behavior in a magnetic field. The computed dipole moment values for the 2-chloro-1-fluoro-4-nitrobenzene molecule are approximately 2.8412 Debye at DFT/B3LYP//6-311++G(d,p) basis set and 2.9382 Debye at HF/6-311++G(d,p) (HF), indicating a polar structure with non-uniform atomic charge distributions, consistent with simulation analyses.

Besides, the compound with the combination of great stability/bioactivity and high dipole moment seems to be useful for the functionalization of the newly synthesized molecules to develop fungicides. Extensive studies have examined how external magnetic fields influence properties such as in vitro regeneration, phenolic content, growth, antioxidant activity, and defense enzyme responses in organic compounds (Ulgen et al., 2020, 2021).

Table 7. Total energies (a.u.), Zero-point correction (a.u./Particle), zero-point vibrational energies (kcal mol⁻¹), entropies (cal mol⁻¹K⁻¹), thermal energies (kcal mol⁻¹), rotational constants (GHz), heat capacities (cal mol⁻¹K⁻¹), and dipole moment (Debye), and Zero-point corrections (a.u./Particle).

Parameters	DFT/B3LYP/ $/6$ -311++(d,p)	HF/6-311++(d,p)
Zero-point vibrational energy	52.078759764	51.2612766
Zero-point correction	0.084652	0.091787
Thermal correction to Energy	0.093559	0.100121
Thermal correction to Enthalpy	0.094503	0.101066
Thermal correction to Gibbs Free Energy	0.049235	0.056877
Sum of electronic and zero-point Energies	-995.673122	-991.988176
Sum of electronic and thermal Energies	-995.664215	-991.979842
Sum of electronic and thermal Enthalpies	-995.663271	-991.978897
Sum of electronic and thermal Free Energies	-995.708539	-992.023086
Total energy	-995.75777428	-992.07996302

Table 7. (continued).

Parameters	DFT/B3LYP//6-311++(d,p)	HF/6-311++(d,p)
	1.84572	1.88353
Rotational constant	0.60797	0.62104
	0.45733	0.46705
Entropy		
Total	95.275	93.003
Translational	41.386	41.386
Rotational	30.816	30.754
Vibrational	23.072	20.863
Heat capacity		
Total	32.620	30.311
Translational	2.981	2.981
Rotational	2.981	2.981
Vibrational	26.659	24.350
Thermal energy		
Total	58.709	62.827
Translational	0.889	0.889
Rotational	0.889	0.889
Vibrational	56.932	61.050
Dipole moment		
μ_{x}	-2.0792	-2.0014
$\mu_{ m y}$	1.9363	2.1511
μ_{z}	0.0000	0.0000
μ	2.8412	2.9382

This section examines the basic properties of frontier molecular orbitals, namely HOMO and LUMO. The HOMO is considered the outermost orbital that contains electrons and acts as an electron donor, while the LUMO is the innermost orbital that has vacancies that can accept electrons (Gece, 2008). Orbitals are crucial to understanding the chemical reactivity and electronic properties of organic molecules. According to molecular orbital theory, interactions between HOMO and LUMO involve electronic transitions such as π - π * transitions, which directly affect the optical and electronic behavior of a molecule (Fukui, 1982).

The HOMO level is related to the ionization potential, which reflects the tendency of the molecule to donate electrons, whereas the LUMO energy level corresponds to the electron affinity, which represents the capacity of the molecule to accept electrons. The energy gap (ΔE) between HOMO and LUMO, also known as the band gap, is a critical measure of molecular

stability, where a smaller gap indicates greater chemical reactivity and a larger gap indicates greater stability (Lewis et al., 1994). Our calculated values for the frontier orbitals and band gap are presented in Table 8, and 3D visualizations of HOMO and LUMO are shown in Figure 2.

The calculated band gap at B3LYP/6-311++G(d,p) modern calculation level is approximately 0.17286 a.u. while at HF/6-311++G(d,p) basis level it is approximately 0.41342 a.u. The larger HF band gap calculated is due to the nonexistence of electron correlation across the HF quantum mechanical method. In the simulations, HOMO is mainly localized in various regions of the molecule, excluding hydrogen (positively charged), nitrogen, (rarely) oxygen, and an amino group, such as H_7 , H_8 , and amino group, whereas LUMO extends to larger areas of the molecule, excluding atoms such as chlorine and hydrogen atoms.

Table 8. Energy gaps, total electronic energies, and molecular quantities determined from DFT/B3LYP//6-311++G(d,p) and the HF/6-311++G(d,p) levels of theory.

Molecular orbital features	DFT/B3LYP//6-311	++G(d,p)HF/6-311++G(d,p)
E _{HOMO} (a.u.)	-0.29148	-0.38077
E_{LUMO} (a.u.)	-0.11862	0.03265
E _{HIGHEST} (a.u.)	215.75794	219.34911
E _{LOWEST} (a.u.)	-101.58774	-104.86940
Energy bandgap, ΔE (E_{HOMO} - E_{LUMO}) (a.u.) bandgAD, AE EHOMO-ELUMO (8.u.	0.17286	0.41342
Ionization potential (IP=-E _{HOMO})	0.29148	0.38077
Electron affinity (EA=-E _{LUMO})	0.11862	-0.03265
Chemical hardness (η)	0.08643	0.20671
Chemical softness (ζ)	5.1790586	2.418847
Electronegativity (χ)	0.20505	0.174706
Chemical potential (µ)	-0.20505	-0.174706
Electrophilicity index (ψ)	0.243234	0.0738285
Maximum charge transfer index (ΔN_{max} =- μ / η)	2.37244	0.84517439

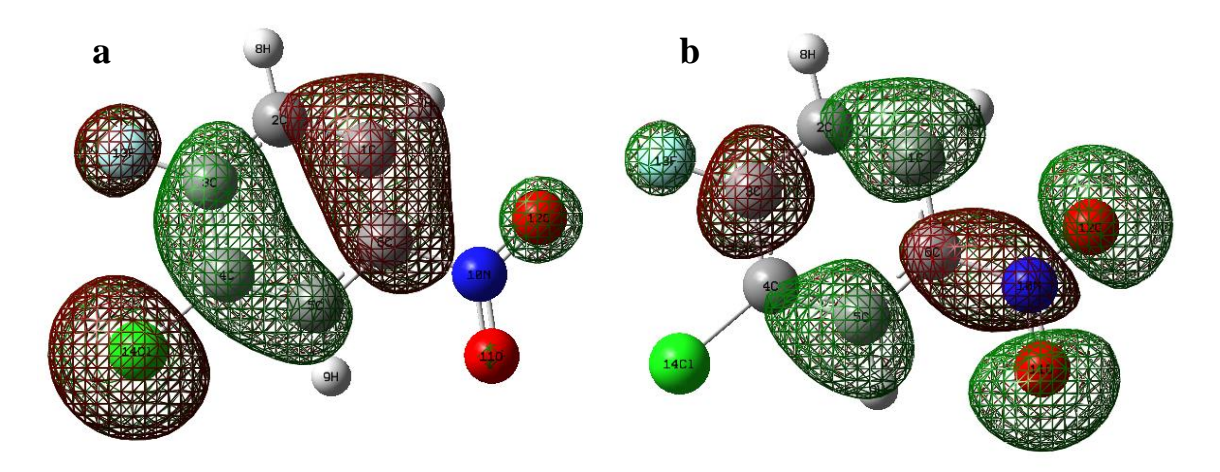


Figure 2. a-) HOMO simulation and b-) LUMO map of the title compound. (Red/green regions reveal the positive/negative phases.

The lowest molecular orbital (MO) eigenvalue for the compound is determined to be -101.58774 a.u. at the B3LYP modern calculation level and -104.86940 a.u at the HF calculation level, while the highest MO eigenvalues are computed as 215.75794 a.u. and 219.34911 a.u. for B3LYPand HF, respectively. These results offer a comprehensive defining of the electronic structure of the 2-chloro-1-fluoro-4-nitrobenzene molecule, demonstrating how stability and reactivity vary with the computational method employed. Furthermore, essential electronic properties such as EA, IP, dipole moment (μ) , softness (ζ) , electronegativity (χ) , electrophilicity (ψ) , hardness (η) , and ΔN_{max} are evaluated through advanced computational chemistry techniques.

This section focuses on the ESP surface map of the title 2-chloro-1-fluoro-4-nitrobenzene compound, providing a detailed view of its molecular size, shape, and charge distribution in its chemical environment. ESP mapping serves as a critical tool for analyzing molecular interactions as it reveals potential reactivity sites and highlights suitable sites for intermolecular and intramolecular interactions such as hydrogen bonding; ESP mapping is consistent with the previously discussed findings on electron density, non-bonding lone pairs, electron engagement, and conjugative effects (Wang et al., 2008).

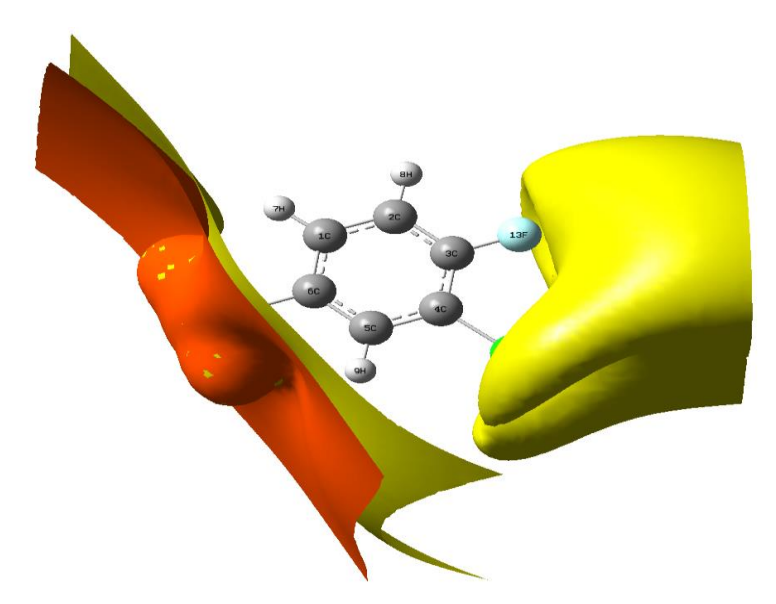


Figure 3. 3D plots of ESP picture of the 2-chloro-1-fluoro-4-nitrobenzene compound.

The map reveals the most negatively charged regions are concentrated round the nitrogen oxide and halogen atoms, indicating that the sites are prone to electrophilic interactions due to the delocalization of their π -electrons. In contrast, other compounds exhibit nucleophilic reactivity sites, highlighting their role as electron-rich sites within the molecule.

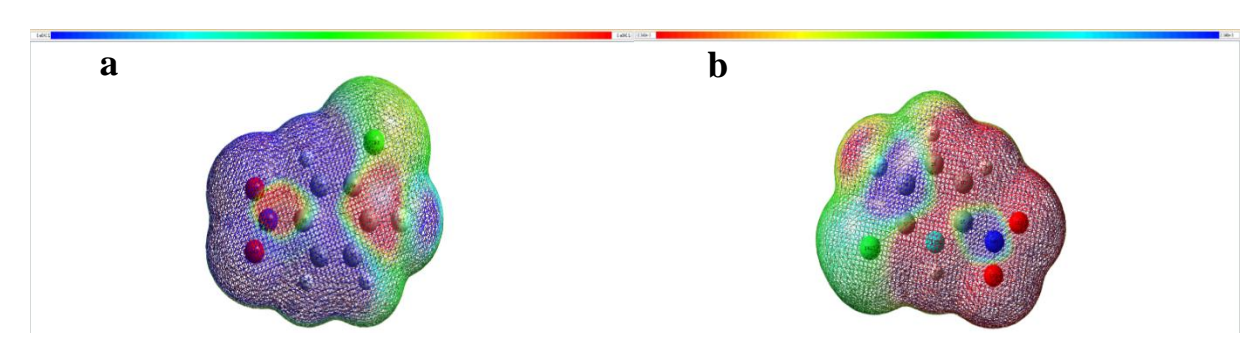


Figure 4. 3D plots of MEP image belonging to 2-chloro-1-fluoro-4-nitrobenzene molecule.

Additionally, the MEP image, which maps the interaction energy between the electron and nuclear charges with a hypothetical positive test charge, is simulated (from both sides) for the molecule and depicted in Figure 4a-b. The MEP image serves as an essential indicator of chemical reactivity by reflecting electron density distribution and revealing areas prone to electrophilic and nucleophilic attacks, as well as potential hydrogen-bonding sites (Politzer & Murray, 2002). The image of MEP extends to understanding how external magnetic fields influence biological and chemical properties, such as in vitro regeneration, phenolic composition, growth, antioxidant activity, and enzymatic defense responses of organic and herbal compounds (Ulgen et al., 2017). The MEP map reveals regions of reactivity, where red areas indicate sites favorable for electrophilic attack and blue areas indicate sites favorable for nucleophilic reactivity. The highest negative potentials, indicating electrophilic reactivity, are concentrated around certain carbon and nitrogen atoms, while positive potentials, indicating nucleophilic behavior, are seen around

bromine and hydrogen atoms. In this respect, the MEP findings demonstrate the complex reactivity profile of the 3-chloro-4-fluoronitrobenzene molecule, capable of engaging in both electrophilic and nucleophilic interactions. The distinct charge distribution further suggests potential for metallic bonding and other intermolecular interactions, underscoring its potential for an extensive range of chemical application fields. In conclusion, the simulations obtained for the 2-chloro-1-fluoro-4-nitrobenzene molecule indicate clearly that the compound with high reactive parts is ideal for the advanced applied sciences.

5. Conclusion

In the current work, we try to define the reactivity and stability of the 3-chloro-4-fluoronitrobenzene molecule for the future application fields as regards advanced applied sciences, physics, industry, chemistry, biology, medicine, pharmaceuticals, dyes, and agrochemicals of the compound, we

make some calculations including vibrational frequencies, dipole moments, related assignments of vibrations, optimized molecular structures, atomic charge distributions, ICT regions, thermodynamic properties at 300 K, UV-vis absorption functional identifications, maxima, group electrophilic/nucleophilic aromatic regions, charge transfer characteristics, lone (non-bonding) pairs, chemical hardness, energy band gap, molecular softness, and electronegativity NMR chemical shifts, conjugation of π bonds, and electron engagement regions. Besides, we simulate, for the first time, 2D total charge contours, MEP, LUMO, ESP, and HOMO images of the 3-chloro-4-fluoronitrobenzene compound. We also compare the NMR and FTIR spectra with the theoretical computations. According to the comparisons, the calculations are closely aligned with experimental ones. The findings also reveal that the compound possesses high ICT regions, lone pairs, electron-donating groups, π -bond conjugation, and especially electrophilic/nucleophilic aromatic regions. This points out that the material has a potential for metallic bonding and intermolecular interactions. Overall, this study not only aids in the identification of the molecule analyzed but also provides valuable insights for researchers, supporting both foundational research and practical applications in technology and industry.

Conflict of Interest

The authors declare that they have no conflict of interest.

References

- Altunpak, Y., Yaşar, M., & Önal, M., (2019). Electrical sliding wear behaviour of an aged high conductivity cu-be alloy. *IOSR Journal of Engineering*, 09(11), 53-60.
- Avci, D., & Atalay, Y. (2009). Theoretical analysis of vibrational spectra and scaling-factor of 2-aryl-1, 3, 4-oxadiazole derivatives. *International Journal of Quantum Chemistry*, 109(2), 328-341. https://doi.org/10.1002/qua.21789
- Baraistka, H., Labudzinska, A., & Terpinski, J. (1987). Laser Raman spectroscopy: Analytical applications (Series: Ellis Horwood series in analytical chemistry). Ellis Harwood Publishers.
- Becke, A. D. (1992). Density-functional thermochemistry. I. The effect of the exchange-only gradient correction. *The Journal of Chemical Physics*, 96(3), 2155-2160. https://doi.org/10.1063/1.462066
- Buyukuslu, H., Akdogan, M., Yildirim, G., & Parlak, C. (2010). Ab initio Hartree-Fock and density functional theory study on characterization of 3-(5-methylthiazol-2-yldiazenyl)-2-phenyl-1H-indole. Spectrochimica Acta Part A: Molecular and Biomolecular Spectroscopy, 75(4), 1362-1369. https://doi.org/10.1016/j.saa.2010.01.003

- Chen, J., & Wang, H. (2021). Density, viscosity, and saturated vapour pressure of 3-chloro-4-fluoronitrobenzene and 3-chloro-2-fluoronitrobenzene. *The Journal of Chemical Thermodynamics*, *154*, 106337. https://doi.org/10.1016/j.jct.2020.106337
- Coates, J. (2006). Interpretation of infrared spectra, a practical approach. *Encyclopedia of Analytical Chemistry: Applications, Theory and Instrumentation*, 12, 10815-10837. https://doi.org/10.1002/9780470027318.a5606
- Dennington, R., Keith, T., & Millam, J. (2007). *GaussView, Version 4.1.2*. Semichem Inc., Shawnee Mission.
- Ertem, A. G., & Altunpak, Y. (2019). Effect of electrode materials type on resistance spot welding of AISI 304 austenitic stainless steel (ASS) sheets. *International Journal for Research in Applied Science and Engineering Technology*, 7(11), 280-284. https://doi.org/10.22214/ijraset.2019.11045
- Fogarasi, G., & Pulay, P. (1986). Quantum chemical calculation of force constants and vibrational spectra. *Journal of Molecular Structure*, *141*, 145-152. https://doi.org/10.1016/0022-2860(86)80318-0
- Fogarasi, G., Zhou, X., Taylor, P. W., & Pulay, P. (1992). The calculation of ab initio molecular geometries: Efficient optimization by natural internal coordinates and empirical correction by offset forces. *Journal of the American Chemical Society*, *114*(21), 8191-8201. https://doi.org/10.1021/ja00047a032
- Foresman, J., & Frish, E. (1996). *Exploring chemistry with electronic structure methods*. Gaussian Inc.
- Fukui, K. (1982). Role of frontier orbitals in chemical reactions. *Science*, 218, 747-754. https://doi.org/10.1126/science.218.4574.747
- Furche, F., & Ahlrichs, R. (2002). Adiabatic time-dependent density functional methods for excited state properties. *The Journal of Chemical Physics*, *117*(16), 7433-7447. https://doi.org/10.1063/1.1508368
- Gece, G. (2008). The use of quantum chemical methods in corrosion inhibitor studies. *Corrosion Science*, 50(11), 2981-2992. https://doi.org/10.1016/j.corsci.2008.08.043
- Helgaker, T. U., Jensen, H. J. R. A., & Jørgensen, P. (1986). Analytical calculation of MCSCF dipole-moment derivatives. *The Journal of Chemical Physics*, 84(11), 6280-6284. https://doi.org/10.1063/1.450772
- Keresztury, G., Holly, S., Besenyei, G., Varga, J., Wang, A., & Durig, J. R. (1993). Vibrational spectra of monothiocarbamates-II. IR and Raman spectra, vibrational assignment, conformational analysis and ab initio calculations of S-methyl-N, N-dimethylthiocarbamate. Spectrochimica Acta Part A: Molecular Spectroscopy, 49(13-14), 2007-2026. https://doi.org/10.1016/S0584-8539(09)91012-1

- Kikuchi, M., Nakagawa, M., Tone, S., Saito, H., Niino, T., Nagasawa, N., & Sawai, J. (2016). Predicting changes in aquatic toxicity of chemicals resulting from solvent or dispersant use as vehicle. *Chemosphere*, *154*, 34-39. https://doi.org/10.1016/j.chemosphere.2016.03.030
- Kohn, W., Becke, A. D., & Parr, R. G. (1996). Density functional theory of electronic structure. *The Journal of Physical Chemistry*, *100*(31), 12974-12980. https://doi.org/10.1021/jp9606691
- Krishnakumar, V., Prabavathi, N., & Muthunatesan, S. (2008).

 Density functional theory calculations and vibrational spectra of 6-methyl 1, 2, 3, 4-tetrahyroquinoline. *Spectrochimica Acta Part A: Molecular and Biomolecular Spectroscopy*, 69(3), 853-859. https://doi.org/10.1016/j.saa.2007.05.034
- Lewis, D. F. V., Ioannides, C., & Parke, D. V. (1994). Interaction of a series of nitriles with the alcohol-inducible isoform of P450: Computer analysis of structure—activity relationships. *Xenobiotica*, 24(5), 401-408. https://doi.org/10.3109/00498259409043243
- Morikawa, A., Furukawa, T. A., & Moriyama, Y. (2005). Synthesis and characterization of novel aromatic polyimides from bis (4-amino-2-biphenyl) ether and aromatic tetracarboxylic dianhydrides. *Polymer Journal*, 37(10), 759-766. https://doi.org/10.1295/polymj.37.759
- Olsen, J., & Jørgensen, P. (1985). Linear and nonlinear response functions for an exact state and for an MCSCF state. *The Journal of Chemical Physics*, 82(7), 3235-3264. https://doi.org/10.1063/1.448223
- Polavarapu, P. L. (1990). Ab initio vibrational Raman and Raman optical activity spectra. *Journal of Physical Chemistry*, 94(21), 8106-8112. https://doi.org/10.1021/j100384a024
- Politzer, P., & Abu-Awwad, F. (1998). A comparative analysis of Hartree-Fock and Kohn-Sham orbital energies. *Theoretical Chemistry Accounts*, 99, 83-87. https://doi.org/10.1007/s002140050307
- Politzer, P., & Murray, J. S. (2002). The fundamental nature and role of the electrostatic potential in atoms and molecules. *Theoretical Chemistry Accounts*, 108, 134-142. https://doi.org/10.1007/s00214-002-0363-9
- Pulay, P., Fogarasi, G., Pongor, G., Boggs, J. E., & Vargha, A. (1983). Combination of theoretical ab initio and experimental information to obtain reliable harmonic force constants. Scaled quantum mechanical (QM) force fields for glyoxal, acrolein, butadiene, formaldehyde, and ethylene. *Journal of the American Chemical Society*, 105(24), 7037-7047. https://doi.org/10.1021/ja00362a005
- Rauhut, G., & Pulay, P. (1995). Transferable scaling factors for density functional derived vibrational force fields. *The Journal of Physical Chemistry*, 99(10), 3093-3100. https://doi.org/10.1021/j100010a019

- Ravi, R., Sivaramakrishnan, H., & Nagarajan, K. (1997).

 Nucleophilic substitutions on 3-chroro-4fluoronitrobenzene. *Indian Journal of Chemistry*Section B-Organic Chemistry Including Medicinal
 Chemistry, 36(4), 347-348.
- Rintoul, L., Micallef, A. S., & Bottle, S. E. (2008). The vibrational group frequency of the N–O stretching band of nitroxide stable free radicals. *Spectrochimica Acta Part A: Molecular and Biomolecular Spectroscopy*, 70(4), 713-717. https://doi.org/10.1016/j.saa.2007.08.017
- Saiardi, A., Erdjument-Bromage, H., Snowman, A. M., Tempst, P., & Snyder, S. H. (1999). Synthesis of diphosphoinositol pentakisphosphate by a newly identified family of higher inositol polyphosphate kinases. *Current Biology*, *9*(22), 1323-1326. https://doi.org/10.1016/S0960-9822(00)80055-X
- Schell, M. J., Letcher, A. J., Brearley, C. A., Biber, J., Murer, H., & Irvine, R. F. (1999). PiUS (Pi uptake stimulator) is an inositol hexakisphosphate kinase. *FEBS Letters*, 461(3), 169-172. https://doi.org/10.1016/S0014-5793(99)01462-3
- SDBS. (2024). Spectral database for organic compounds, SDBS. https://sdbs.db.aist.go.jp/
- Spencer, J., Rathnam, R. P., Patel, H., & Anjum, N. (2008). Microwave mediated reduction of heterocycle and fluorine containing nitroaromatics with Mo (CO) 6 and DBU. *Tetrahedron*, 64(44), 10195-10200. https://doi.org/10.1016/j.tet.2008.08.036
- Stephens, P. J., Devlin, F. J., Chabalowski, C. F., & Frisch, M. J. (1994). Ab initio calculation of vibrational absorption and circular dichroism spectra using density functional force fields. *The Journal of Physical Chemistry*, *98*(45), 11623-11627. https://doi.org/10.1021/j100096a001
- Ulgen, C., Yıldırım, A. B., & Turker, A. U. (2017). Effect of magnetic field treatments on seed germination of melissa officinalis L. *International Journal of Secondary Metabolite*, 4(3, Special Issue 1), 43-49. https://doi.org/10.21448/ijsm.356283
- Ulgen, C., Yıldırım, A., & Turker, A. (2020). Enhancement of plant regeneration in lemon balm (*Melissa officinalis* L.) with different magnetic field applications. *International Journal of Secondary Metabolite*, 7(2), 99-108. https://doi.org/10.21448/ijsm.677102
- Ulgen, C., Yildirim, A. B., Sahin, G., & Turker, A. U. (2021). Do magnetic field applications affect in vitro regeneration, growth, phenolic profiles, antioxidant potential and defense enzyme activities (SOD, CAT and PAL) in lemon balm (*Melissa officinalis* L.). *Industrial Crops and Products*, 169, 113624 https://doi.org/10.1016/j.indcrop.2021.113624
- Wang, D. L., Sun, X. P., Shen, H. T., Hou, D. Y., & Zhai, Y. C. (2008). A comparative study of the electrostatic potential of fullerene-like structures of Au₃₂ and Au₄₂.

- *Chemical Physics Letters*, *457*(4-6), 366-370. https://doi.org/10.1016/j.cplett.2008.04.038
- Wilson, E. B., Decius, J. C., & Cross, P. C. (1980). *Molecular vibrations: The theory of infrared and Raman vibrational spectra*. Courier Corporation.
- Wojtkowiak, B., & Chabanel, M. (1977). *Spectrochimie moléculaire*. Paris: Technique et documentation. (In French)
- Wu, Q., & Yang, W. (2002). Empirical correction to density functional theory for van der Waals interactions. *The Journal of Chemical Physics*, *116*(2), 515-524. https://doi.org/10.1063/1.1424928
- Zhang, Y., Ma, Z., Yang, M., Chen, Y., Tang, B., & Zhu, T. (2024). Preparation of modified graphyne to detect genotoxic impurities in gefitinib: Effects of ionic liquid structures and carbon nanotube composite modes. *Microchemical Journal*, 201, 110651. https://doi.org/10.1016/j.microc.2024.110651